Carbohydrate Polymers 81 (2010) 572–577

Contents lists available at ScienceDirect

Carbohydrate Polymers

journal homepage: www.elsevier.com/locate/carbpol

Structure of rhamnan sulfate from the green alga *Monostroma nitidum* and its anti-herpetic effect

Jung-Bum Lee*, Seiji Koizumi, Kyoko Hayashi, Toshimitsu Hayashi

Graduate School of Medicine and Pharmaceutical Sciences for Research, University of Toyama, 2630 Sugitani, Toyama 930-0194, Japan

ARTICLE INFO

Article history:
Received 10 February 2010
Received in revised form 24 February 2010
Accepted 5 March 2010
Available online 12 March 2010

Keywords:
Rhamnan sulfate
Monostroma nitidum
Antiviral activity
Herpes simplex virus type 2

ABSTRACT

"A sulfated polysaccharide from *Monostroma nitidum* Wittrock (Ulvophyceae)" was purified by anion-exchange and gel filtration column chromatographies. The isolated polysaccharide consisted of large amount of L-rhamnose with small amount of D-glucose, and it was regarded to be a rhamnan sulfate (RS). Methylation analysis of the native and desulfated polysaccharide suggested that this polymer was mainly composed of 1,2- and 1,3-linked rhamnose residues with a ratio of *ca* 1:2. In addition, it was found the presence of 1,2,3-linked rhamnose and 1,4-linked glucose residues. Sulfate groups were suggested to be mainly located at C-2 and C-3 of 1,3- and 1,2-linked rhamnose residues, respectively. NMR analyses including 1D and 2D experiments indicated that RS consisted of sugar linkage units as follows:

1: →3)-α-L-Rha-(1 → 3)-α-L-Rha-(1→
2: →3)-α-L-Rha-(1 → 2)-α-L-Rha-(1→
3: →3)-α-L-Rha-(1 → 3)-α-L-Rha-(1→

2
β-D-Glc-(1- ↑

Moreover, RS showed potent antiviral activity against herpes simplex virus type 2 virus, whereas it has no effect on the replication of influenza A virus. Anti-HSV-2 target(s) of RS was suggested to be virus adsorption and penetration steps onto host cell surface.

1. Introduction

Herpes simplex virus type 2 (HSV-2) is an ubiquitous pathogen and major cause of genital herpes. Immunocompetent people with genital HSV infection can have frequent, painful, and recurrent genital lesions associated with much psychosocial distress. Over the past two decades, HSV-2 infection has also been linked to three times higher risk of sexually acquired HIV (Freeman et al., 2006). Therefore, treatment and prophylaxis of the infection of HSV-2 should reduce the likelihood of HIV infection. Acyclovir is the most commonly used chemotherapy as a very effective treatment for HSVs, however, it is not always tolerated and drug-resistant mutants are rapidly emerging, particularly in immunocompromised patients. Thus, it is demanded to develop novel type of anti-HSV drugs with novel mode of action.

So far, many polysaccharides from algae have been studied vigorously on their structures and biological activities. In especial, fucoidans (fucan sulfates) from brown algae have been focused on those studies, because they have various biological activities such as anticoagulant and antiviral activities (Berteau & Mulloy, 2003; Hayashi, Nakano, Hashimoto, Kanekiyo, & Hayashi, 2008; Hoshino et al., 1998). On the other hand, some algae produce specific sulfated polysaccharides which are mainly composed of α-L-rhamnose moiety. An α-L-rhamnose is a rare monosaccharide in human and animals, whereas it is widely distributed in plants and microorganisms as a component of glycosides or polysaccharides. However, distribution of a polymer composed of large amounts of α-L-rhamnose, so-called "rhamnan", is quite limited in the nature. Our studies have demonstrated that some rhamnan-type sulfated polysaccharides, such as sodium spirulan (Na-SP) from *Spirulina platensis* (cyanophyta) and rhamnan sulfate (RS) from *Monostroma latissimum* (chlorophyta), had potent antiviral activities against enveloped viruses including human immunodeficiency virus type 1 (HIV-1) and herpes simplex viruses (HSVs) (Hayashi & Hayashi, 1996; Lee, Hayashi, Hayashi, Sankawa, & Maeda, 1999). The green alga *M. nitidum* grows in upper part of intertidal zone, and widely cultivated to use as food resources at Mie and Oki-

* Corresponding author at: Laboratory of Phamacognosy, Graduate School of Medicine and Pharmaceutical Sciences for Research, University of Toyama, Japan. Tel.: +81 76 434 7580; fax: +81 76 434 5170.
E-mail address: lee@pha.u-toyama.ac.jp (J.-B. Lee).

0144-8617/$ – see front matter © 2010 Elsevier Ltd. All rights reserved.
doi:10.1016/j.carbpol.2010.03.014

nawa in Japan. There are several reports about the structure of sulfated polysaccharides from *Monostroma* sp. (Harada & Maeda, 1998; Lee, Yamagaki, Maeda, & Nakanishi, 1998), however, fine chemical structure of rhamnan sulfate from *Monostroma* sp. is not elucidated. In the present paper, we describe the fine structural investigations of the sulfated rhamnan from *M. nitidum* and the evaluation of their antiviral activities.

2. Materials and methods

2.1. Isolation of rhamnan sulfate

Crude rhamnan sulfate (CRS) extracted from *Monostroma nitidum* was kindly gifted from Mr. Shigeo Tanaka (Konan Chemical Manufacturing Co., Ltd., Mie, Japan). Briefly, dried seaweed was washed with H_2O and then extracted with 24 vol. of H_2O for 6 h at 95–100 °C. Then, celite (300 g) was added to the extract, and then centrifuged to remove algal fronds. Thus obtained hot water extract was lyophilized to give CRS (153 g). CRS (45 g) dissolved in H_2O was dialyzed against H_2O to fractionate to dialyzate (ML) and non-dialyzate (MH) fractions, and then both were freeze-dried (Yield: ML, 13.5 g; MH, 26.1 g). MH was dissolved in H_2O and applied to a Toyopearl DEAE 650 M anion-exchange chromatography (5 i.d. × 14 cm; Tosoh, Tokyo, Japan), which was successively eluted with H_2O, 0.5 M NaCl, 1.0 M NaCl, and 2.0 M NaCl. The yields of the eluates were 23 (MH-1), 13 (MH-2), 32 (MH-3), and 3% (MH-4), respectively. MH-3 obtained as the most abundant fraction was applied to a Toyopearl DEAE 650 M column (5 i.d. × 14 cm), which was eluted with a linear gradient system prepared by H_2O and 1.5 M NaCl. Fractions of 20 ml were collected and monitored by the phenol–H_2SO_4 method (Dubois, Gilles, Hamilton, Revers, & Smith, 1956) and UV detection at 280 nm. MH-3A (3%), MH-3B (25%), MH-3C (41%), and MH-3D (14%) were obtained on the basis of their elution profiles. The most abundant fraction, MH-3C, was applied to a Toyopearl HW-65S gel filtration (2.2 i.d. × 96.5 cm) and eluted with 0.1 M NaCl. Fractions of 5 ml were collected and monitored by the phenol–H_2SO_4 method to obtain a rhamnan sulfate (RS, yield = 62.5%).

2.2. Estimation of homogeneity of RS

The molecular weight of RS was estimated by HPLC analysis. The sample was applied on TSK $GMPW_{XL}$ gel filtration columns (7.6 mm × 300 mm × 2; Tosoh, Tokyo, Japan) and eluted with 0.1 M $NaNO_3$ at 0.6 ml/min. Commercially available pullulans (Shodex P-52; Showa Denko K.K., Tokyo, Japan) were used as standard molecular markers. RS was applied to a cellulose-acetate membrane (Separax; Jokoh Co. Ltd., Tokyo, Japan) in 0.1 M barium acetate and run at 1 mA/cm. The membrane was stained with 0.25% toluidine blue.

2.3. Colorimetric analyses of polysaccharide

Uronic acid content was determined by *m*-hydroxydiphenyl method (Blumenkrantz & Asboe-Hansen, 1973). Protein content was determined using a Bio-Rad protein assay kit. Sulfate content was determined by rhodizonate method (Silvestri, Hurst, Simpson, & Settine, 1982).

2.4. Sugar composition of RS

Sugar composition was determined as follows: RS (1 mg) was hydrolyzed with 2 M trifluoroacetic acid (TFA) at 120 °C for 1 h. After removal of TFA under N_2 gas, the hydrolyzates were converted to alditol acetates, which were analyzed by GC using a SP-2330 fused silica capillary column (30 m × 0.32 mm i.d.; Supelco, MA, USA) with the oven temperature of 200–240 °C (4 °C/min). Absolute configuration of monosaccharide was analyzed as (+)-2-butyl-glycoside (Gerwig, Kamerling, & Vliegenthart, 1979).

2.5. Methylation analyses of polysaccharides

Desulfation of RS was performed by solvolytic desulfation with 10% MeOH/DMSO (Nagasawa, Inoue, & Tokuyasu, 1979). After dialysis and lyophilization, a colorless polysaccharide was obtained (DS-RS). RS was converted to the triethylammonium salt (TEA-RS) by dialyzed against 0.1 M triethylammonium hydrogen chloride (Stevenson & Furneaux, 1991). Methylation of TEA-RS and DS-RS was performed by the Ciucanu's method (Ciucanu & Kerek, 1984). In the case of TEA-RS, it was methylated three times to achieve complete methylation. The methylated polysaccharides were hydrolyzed with 2 M TFA at 120 °C for 1 h, reduced with $NaBD_4$, and acetylated. The partially methylated alditol acetates were analyzed GC using a SP-2330 fused silica capillary column and GC–MS using a DB-5MS fused silica capillary column. Identification of partially methylated alditol acetates was carried out on the basis of relative retention time to 1,5-di-*O*-acetyl-2,3,4,6-tetra-*O*-methylglucitol and its mass fragmentation patterns (Carpita & Shea, 1988). Peak area was corrected using published molar response factors (Sweet, Shapiro, & Albersheim, 1975).

2.6. Spectroscopic analyses of polysaccharides

IR spectra of RS and DS-RS were recorded with a FT/IR-460plus spectrophotometer (Jasco, Tokyo, Japan). NMR spectra were recorded at 303 K on a Varian Unity 500 *plus* spectrophotometer, and sodium 2,2-dimethyl-2-silapentane-5-sulfonate (DSS) was used as internal reference. The homonuclear two-dimensional experiments such as DQF-COSY, TOCSY (spinlock time of 80 ms), NOESY (mixing time of 80 ms) were performed using the Varian standard program. The heteronuclear experiments were performed using pulse field gradient program as gHSQC, gHSQC-TOCSY, and gHMBC. H2BC experiments were performed with reported pulse program (Petersen et al., 2006).

2.7. Cells and viruses

Vero and MDCK cells were grown in Eagle's MEM supplemented with 5% FBS and kanamycin (60 mg/l). RAW 264.7 cells were grown in DMEM supplemented with 10% FBS. HSV-2 (UW268 strain) and influenza A virus (A/NWS/33 strain, H1N1) were propagated on Vero and MDCK cells, respectively. Those viruses were stored at −80 °C until use. An aliquot of the virus stock was titered by plaque assay.

2.8. Antiviral activity and cytotoxicity of RS

Vero and MDCK cell monolayers (2×10^5 cells/well) were infected with HSV-2 or influenza virus, respectively, at 0.1 plaque forming unit (PFU) per cell at room temperature. After 1 h of viral infection, the monolayers were washed three times with phosphate-buffered saline (PBS) and incubated in a maintenance medium (MEM plus 2% FBS) at 37 °C. Sample was added either during infection and throughout the incubation thereafter (A) or immediately after the viral infection (B). Virus yields were determined by plaque assay at 1-day incubation point. The 50% inhibitory concentration (IC_{50}) was obtained from concentration–response curves. For cell growth inhibition study, Vero or MDCK cells were incubated at an initial density of 1.2×10^4 cells/well in 96-well plates. After cells had been incubated for 1 day at 37 °C, sample was added and the incubation was continued for 3 days.

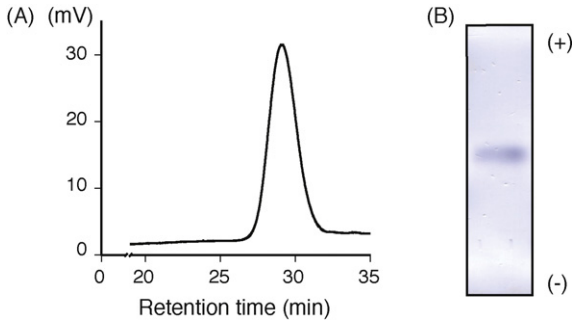

Fig. 1. HPLC and cellulose acetate membrane electrophoresis of RS. (A) HPLC analysis was performed with a TSK-gel $GMPW_{XL}$ column (7.6 mm × 300 mm × 2) at 0.6 ml/min of 0.1 M $NaNO_3$ and peak was monitored by RI detector. (B) Electrophoresis was performed on a cellulose acetate membrane in 0.2 M barium acetate. Polysaccharide was stained with 0.5% toluidine blue.

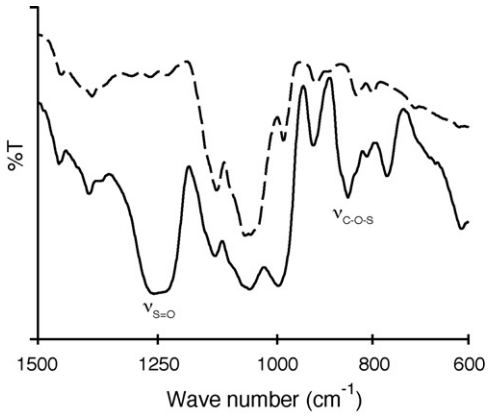

Fig. 2. IR spectrum of RS (solid line) and DSRS (dashed line).

Viable cell yield was determined by the trypan blue exclusion test. The 50% cytotoxic concentration (CC_{50}) was obtained from concentration–response curves. All date were expressed as mean ± SD from triplicate assays.

2.9. Time-of-addition experiments of RS

Vero cell monolayers in 48-well plates were infected with HSV-2 at 10 PFU/cell for 1 h at room temperature. Various concentrations of RS (0.2–500 μg/ml) were added for 1 h before infection (pretreatment), during infection for 1 h, during infection and throughout the incubation thereafter, or after 1, 3, 6, and 8 h following infection. After 20 h incubation, cell cultures were subjected to the plaque assay as mentioned above.

2.10. NO production of RS

Accumulated nitrite, which is a stable oxidized products of NO, in the culture media of RAW 264.7 cells was measured using a colorimetric assay based on the Griess reaction (Green et al., 1982). Briefly, the cells (2×10^5) were seeded in a 96-well plate and incubated in the absence or presence of sample at 37 °C for 24 h. The culture supernatants were reacted with Griess reagent at room temperature for 10 min, and then nitrite concentration was determined by measuring the absorbance at 550 nm. The standard curve was obtained using the known concentrations of sodium nitrite.

3. Results

3.1. Isolation of rhamnan sulfate

CRS was dialyzed against H_2O to fractionate to non-dialyzate (CRS-H) and dialyzate (CRS-L). CRS-H was applied to a DEAE 650 M anion-exchange column chromatography and fractionated into four fractions. Among the fractions, MH-3 eluted with 1 M NaCl, which was the most abundant fraction, was subjected to anion-exchange column chromatography on DEAE 650 M with linear gradient elution. The most abundant fraction (MH-3C) was collected and separated by gel filtration on Toyopearl HW-65S. Analytical GFC showed that the obtained polysaccharide was eluted as a single peak (Mw: 2.03×10^4) and its polydispersity (Mw/Mn) was 1.39 (Fig. 1A). On the other hand, migration pattern of the polysaccharide on cellulose acetate membrane electrophoresis was also single band (Fig. 1B). These results revealed that the obtained polysaccharide might be a homogeneous polysaccharide on the basis of molecular weight and charge distribution, and it was named rhamnan sulfate.

3.2. Chemical characterization of RS

Bradford assay revealed that RS did not contain a protein portion since no color was developed. Small amount of uronic acid was detected by the *m*-hydroxydiphenyl method (4.6%). The IR spectrum indicated the presence of sulfate group since the S=O (1259 cm^{-1}) and the C—O—S (851 cm^{-1}) stretching absorptions (Fig. 2), and they were disappeared after desulfation of RS. By the rhodizonate assay, which is colorimetric assay for sulfate, sulfate content was estimated to contain about 31.7%. From the analysis of neutral sugar composition by the conversion of the hydrolyzates into alditol acetates and (+)-2-butyl glycosides, RS-A was found to be consist of L-rhamnose with trace amounts of D-glucose and D-xylose. Uronic acid residue in RS was revealed to be D-glucuronic acid. In general, methylation analysis is useful to make clear the linkage and sulfate substitution position of sugar residues by comparing the results of native and desulfated polysaccharides. As shown in Table 1, DS-RS contained 2-substituted and 3-substituted rhamnose residues as the main sugar components. In addition, small amounts of disubstituted rhamnose residues and 4-substituted glucose residue were also detected. Therefore, this polysaccharide was suggested to be mainly composed of 1,2- and 1,3-linked rhamnose residues with small amounts of branch. On the other hand, it was found that native polysaccharide consisted of 2-substituted, 3-substituted, and 2,3-disubstituted rhamnose residues. On comparison of data of methylation analysis of native and desulfated polysaccharides, 2,3-disubstituted residue increased, whereas, 2- and 3-substituted residues decreased. Therefore, sulfate groups were suggested to be substituted at C-3 of 1,2-linked and at C-2 of 1,3-linked rhamnose residues.

3.3. NMR analyses of RS and DSRS

The ^1H one-dimensional spectra of the RS and DS-RS are shown in Fig. 3. Three broad anomeric proton signals (5.30, 5.19 and 5.03 ppm) were observed in the ^1H-NMR spectrum of RS, whereas six anomeric proton signals (5.33, 5.25, 5.20, 5.03, 4.96 and

Table 1
Results of methylation analyses of RS and DSRS.

Methylated sugar	Deduced linkage	RS (mol%)	DSRS (mol%)
2,3,4-Me_3-Rha*	Rha*p*-(1→	2.7	2.3
3,4-Me_2-Rha	→2)-Rha*p*-(1→	22.0	32.2
2,4-Me_2-Rha	→3)-Rha*p*-(1→	44.8	57.7
4-Me-Rha	→2,3)-Rha*p*-(1→	23.2	5.3
3-Me-Rha	→2,4)-Rha*p*-(1→	4.5	1.3
2,3,6-Me_3-Glc	→4)-Glc*p*-(1→	2.8	1.2

* 1,5-di-*O*-acetyl-2,3,4-tri-*O*-methylrhamnitol.

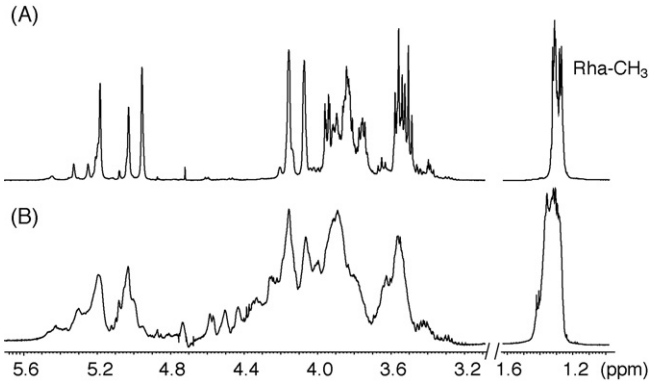

Fig. 3. ^{1}H-NMR spectra of (A) DS-RS and (B) RS. Spectra were recorded in D_2O at 303 K at 500 MHz using 2,2-dimethyl-2-silapentane-5-sulfonate as internal reference.

4.62 ppm) were observed in the case of DS-RS. In the ^{13}C NMR spectrum of DS-RS, the α-anomeric signals attributable to Rha*p* residues were observed in the region of δ 103–105 ppm (Fig. 4). These spectral data were indicative of presence of complex structure in the polysaccharide. Thus, it was suggested that this polysaccharide was arranged in a rather intricate assemblage despite the simplicity of compositional data.

Then, detailed 2D NMR analysis of DS-RS was performed using homo- and heteronuclear experiments in order to obtain information of sugar sequence in the polysaccharide. By combination of several 2D spectra including DQF-COSY, TOCSY, HSQC, HSQC-TOCSY, and H2BC spectra (shown in Supplementary materials), it was possible to assign eleven spin systems, corresponding to different sugar units (Table 2). The assignments of each spin system were made based on HSQC data (Fig. 5A). Residues A to J were all recognized as rhamnose residues as they possessed a small $^{3}J_{H1,H2}$ value and H6/C6 chemical shifts distinctive of a methyl group. On the other hand, spin system K, whose anomeric signals at 4.62 ppm and a $^{3}J_{H1,H2}$ of 8 Hz, was identified as β-glucose residue. By comparison with ^{13}C chemical shifts of α-L-methyl rhamnoside, residue A was suggested to be a 2,3-disubstituted rhamnose residue owing to C-2 and C-3 low field chemical shift (81.9 and 78.9 ppm, respectively). Similarly, it was suggested that residues C and D were 2-substituted residue and residues E, F, G, H, and I were 3-substituted residues.

The sequence of glycosyl residues of DSRS was determined by the interpretation of NOESY and HMBC spectra (Fig. 5B). As summarized in Table 3, strong inter-residual NOE was observed between H-1 of residue A at 5.33 ppm and H-3 of residue G at 3.92 ppm, and long-range correlations between H-1 of residue A and C-3 of residue G was also detected. These results obviously indicated that residue A was linked to 3 position of residue G. H-1 of residue B showed inter-residual NOEs with H-3 of residue A (strong) and I (weak) and long-range correlations with C-3 of residue A and I. Thus, residue B

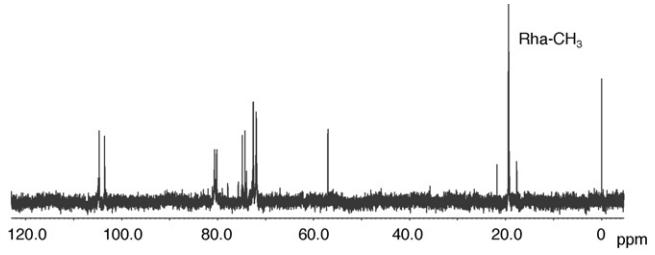

Fig. 4. ^{13}C-NMR spectrum of DS-RS. Spectrum was recorded in D_2O at 303 K at 125 MHz using 2,2-dimethyl-2-silapentane-5-sulfonate as internal reference.

Table 2
^{1}H- and ^{13}C-NMR spectral data of DSRS in D_2O.

Residue	C-1 H-1	C-2 H-2	C-3 H-3	C-4 H-4	C-5 H-5	C-6 H-6
A	103.5 5.33	81.9 4.20	78.9 4.03	74.9 3.65	71.8 3.88	19.6 1.30
B	103.2 5.25	72.7 4.06	n.d. 3.91	74.2 3.56	n.d. n.d.	n.d. n.d.
C	103.4 5.18	80.5 4.07	72.5 3.95	72.8 3.51	71.8 3.83	19.4 1.32
D	103.4 5.20	80.5 4.07	72.5 3.95	72.8 3.51	71.8 3.83	19.4 1.32
E	104.7 5.03	72.6 4.14	81.0 3.90	73.9 3.57	71.9 3.76	19.3 1.28
F	104.7 5.03	72.6 4.14	80.4 3.91	73.9 3.57	71.9 3.76	19.3 1.28
G	104.7 5.03	72.6 4.14	80.6 3.92	73.9 3.57	71.9 3.76	19.3 1.28
H	104.6 4.96	72.5 4.16	80.1 3.85	74.2 3.56	71.9 3.76	19.3 1.27
I	104.6 4.96	72.5 4.16	80.6 3.84	74.2 3.56	71.9 3.76	19.3 1.27
J	104.6 4.96	72.5 4.16	80.3 3.84	74.2 3.56	71.9 3.76	19.3 1.27
K	106.8 4.62	75.6 3.39	77.9 3.53	78.2 3.81	n.d. n.d.	n.d. n.d.
α-MeRha	103.8 4.70	73.0 3.93	73.3 3.71	75.1 3.45	71.4 3.67	19.6 1.31

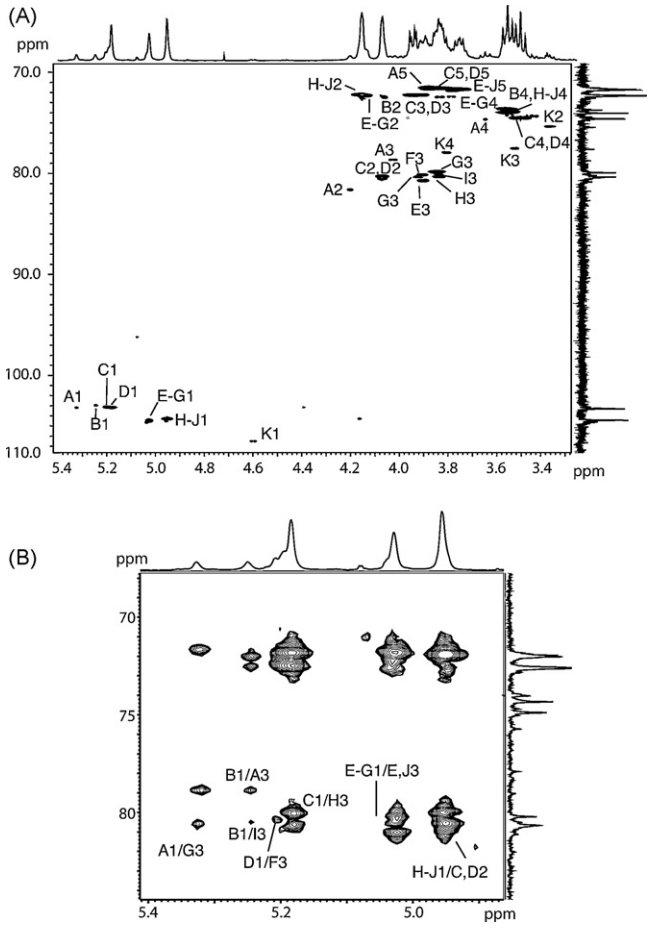

Fig. 5. HSQC (A) and HMBC (B) spectra of DS-RS in which resonances of the eleven different spin systems (A to K) are shown.

Table 3
NOESY and HMBC spectral data of DSRS.

Anomeric proton	NOE contact		Intensity[a]	$J_{C,H}$ Connectivities to	
(*d*, ppm)	(*d*, ppm)			(*d*, ppm)	
A (5.33)	G	H-3 (3.92)	s	G	C-3 (80.6)
B (5.25)	A	H-3 (4.03)	s	A	C-3 (78.9)
	I	H-3 (3.84)	w	I	C-3 (80.6)
C (5.18)	H	H-3 (3.85)	s	H	C-3 (80.1)
D (5.20)	F	H-3 (3.91)	s	F	C-3 (80.4)
E, F, G (5.03)	E	H-3 (3.90)	s	E	C-3 (81.0)
	J	H-3 (3.84)	s	J	C-3 (80.3)
H, I, J (4.96)	C, D	H-2 (4.07)	s	C, D	C-2 (80.5)
K (4.62)	A	H-2 (4.20)	w	A	C-2 (81.9)

[a]The intensities were estimated from visual inspection of NOESY spectra and are given as the following: s = strong and w = weak.
$J_{C,H}$ connectivities for the anomeric atoms (H-1 and C-1) of DSRS.

was suggested to be linked to 3 positions of residue A (major) and residue I (minor). Residue C and D were suggested to be linked at 3 positions of residue H and F, respectively, because they showed intra-residual NOEs and HMBC correlations against H-3 and C-3 of each residue. Residues E, F, and G showed NOEs for H-3 of residue E and J and HMBC correlations for C-3 of those residues. Therefore, those residues was suggested to link at 3 position of residue E or J. H-1 of residue H, I, and J showed inter-residual NOEs for H-2 and HMBC correlations for C-2 of residue C or D, thus the residue was linked at 2 position of residue C or D. Finally, β-Glc residue was linked to 2 position of residue A as shown in Table 3. It was deduced by an inter-residual NOE between the anomeric proton of residue K and the H-3 of the residue A and by the cross peak in the HMBC of the same anomeric proton to C-2 of the residue A.

These spectroscopic assumptions were in full agreement with a rhamnan backbone consisted of 1,2- and 1,3-linked α-Rha residues. These findings could lead to several possible combinations: B-A-G-E, B-A-G-J, C-H, D-F-E, D-F-J, E-E, and E-J. The sequence of B-A-G-E and B-A-G-J revealed that the presence of →3)-α-Rha-(1 → 3)-α-Rha-(1 → 3)-α-Rha-(1 → 3)-α-Rha-(1→, and →4)-β-Glc-(1 → (K) residue was linked to A residue as shown in Fig. 6. The sequence C-H was indicative the presence of →2)-α-Rha-(1 → 3)-α-Rha-(1→, and this sequence was found to connect to the same sequence or residue D. Therefore, it was suggested that the presence of disaccharide repeating unit of →2)-α-Rha-(1 → 3)-α-Rha-(1→. The residue D was found to consist of two sequences, D-F-E and D-F-J, and the both indicated the presence of the intricate unit, →2)-α-Rha-(1 → 3)-α-Rha-(1 → 3)-α-Rha-(1→. The sequences of E-E and E-J were →3)-α-Rha-(1 → 3)-α-Rha-(1→, however, E-E was suggested to connect to the same sequence whereas E-J was connected to D residue. As described above, these sequences also indicated the presence of the intricate sequences.

3.4. Biological activities of RS

As shown in Table 4, RS showed marked antiviral activity against HSV-2, whereas no inhibitory effect was observed on influenza A virus replication. Furthermore, RS showed a low inhibitory effect on

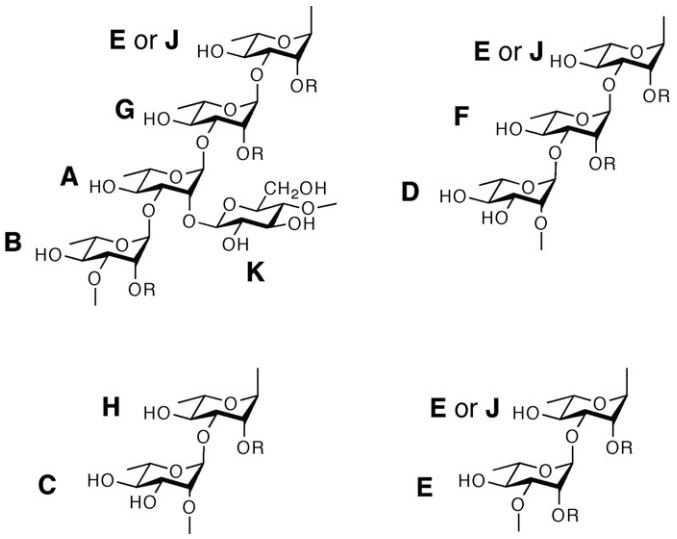

Fig. 6. Intrinsic sugar sequences in RS.

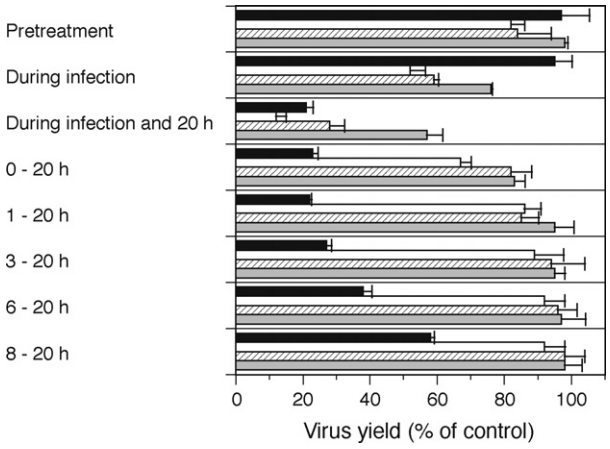

Fig. 7. Time-of-addition experiments of RS. Vero cells were infected with HSV-2 (10 PFU/cell). RS was added to the medium at the indicated time at the concentration of 10 (gray bar), 100 (stripe bar) or 1000 μg/ml (open bar). Acyclovir (10 μg/ml) was used as positive control (closed bar). All data were expressed as mean ± SD of triplicates.

the cell growth, with CC_{50} values being higher than >10,000 μg/ml. When it was added to the medium during infection and throughout the incubation (A) or immediately after viral infection (B), the IC_{50} values against HSV-2 replication were 0.87 and 40 μg/ml, respectively. These findings suggested that the main antiviral target of RS might be virus adsorption and/or penetration step(s) on host cell surface. To delineate the drug-sensitive phase, time-of-addition experiments were carried out (Fig. 7). In these experiments, Vero cells were infected with HSV-2 at a high titer of 10 PFU per cell, and data for samples were compared with those of acyclovir, which is

Table 4
Antiviral activities of RS.

Virus	Host cells	Cytotoxicity	Antiviral activity		Selectivity index	
		(CC_{50}, μg/ml)	(IC_{50}, μg/ml)		(CC_{50}/IC_{50})	
			A*	B	A	B
HSV-2	Vero	>10000	0.87	40	>11000	>250
IFV-A	MDCK	>10000	>1000	>1000	><10	><10

A: Sample was added to the medium during infection and throughout the incubation thereafter.
B: Sample was added to the medium immediately after viral infection.

a clinically used drug. Pretreatment of host cells with RS produced no inhibitory effect on HSV-2 replication, and only low anti-HSV-2 effect was observed when added to the medium during virus infection. On the other hand, dose-dependent inhibitory effect on virus replication was observed when added to the medium at the same time as viral infection for 1 h and throughout the incubation thereafter. However, no antiviral effect was shown when RS was added to the medium after virus infection.

So far, some sulfated polysaccharides from seaweeds have been shown to induce nitric oxide (NO) production (Leiro, Castro, Arranz, & Lamas, 2007; Nakamura, Suzuki, Wada, Kodama, & Doi, 2006). Thus, we evaluated whether RS showed induction of NO production or not. As a result, RS showed no effect of NO production on murine macrophage-like cell line RAW 264.7 cells (data not shown). In addition, RS also did not show immunosuppressive effect on NO production after treatment of cells with LPS (data not shown).

4. Discussion

So far, many sulfated polysaccharides have been isolated from seaweeds and their biological activities were evaluated. Especially, fucoidans from brown seaweeds are exhaustively studied on their biological effects (Berteau & Mulloy, 2003; Kusaykin et al., 2008). On the other hand, a few limited reports on structural elucidation and evaluation of biological activities of sulfated polysaccharides from green seaweeds have been demonstrated. Among them, Harada and Maeda have demonstrated structural features of rhamnan-type sulfated polysaccharides, which mainly consisted of α-1,3-linked L-rhamnose residues, from *M. nitidum* (Harada & Maeda, 1998). However, our rhamnan sulfate from *M. nitidum* was composed of α-1,3-linked and α-1,2-linked rhamnose residues in the ratio of *ca* 2:1. It was suggested that the differences in previous report and our present data might be derived from the distinction of collecting location and date of *M. nitidum*. We also have already experienced that some sulfated polysaccharides, fucan sulfate, showed variation of their chemical structure and physicochemical properties, whereas their biological potencies seemed to be similar (Hoshino et al., 1998; Preeprame, Hayashi, Lee, Sankawa, & Hayashi, 2001). As a conclusion, we have thought that geographical difference and/or time of collection date might presumably influence the characteristics of sulfated polysaccharides. While all data suggested that RS contains three structural units, the rhamnan from *M. nitidum* is not a strictly repetitive polymer. In many cases of sulfated polysaccharides such as heparan sulfate, microheterogeneities within sugar residues and/or sulfation patterns are well recognized, and have been suggested due to sequential enzymatic modifications in the biosynthesis of these molecules (Liu & Pedersen, 2007). Therefore, the complexity of rhamnan backbone structure found in the polysaccharide from *M. nitidum* might be due to its biosynthetic machinery.

Recently, it is paid attention to manage HSV-2 infection because this virus is recognized as one of important risk factor of HIV spread, and co-infection of HSV-2 with HIV leads to changes of HIV tropism (Palú, Benetti, & Calistri, 2001). Therefore, the management of HSV-2 infection is important for the prevention of spread and disease progression. In the present study, RS clearly showed a potent anti-HSV-2 effect (Table 4). Furthermore, time-of-addition experiments revealed that RS might interfere with early step(s) of virus replication cycle such as virus binding onto host cell surface and virus penetration step (Fig. 7).

In summary, we have demonstrated the fine structure of RS isolated from *M. nitidum*. The polysaccharide had anti-HSV-2 activity whereas it showed no effect on the replication of influenza A virus. It was suggested that RS might be a specific inhibitor of HSV-2 adsorption to and penetration into host cells and might be useful as preventive agent for HSV-2 infection.

Acknowledgement

Crude rhamnan sulfated was kindly gifted from Mr. Shigeo Tanaka, Konan Chemical Manufacturing Co. Ltd., Japan.

Appendix A. Supplementary data

Supplementary data associated with this article can be found, in the online version, at doi:10.1016/j.carbpol.2010.03.014.

References

Berteau, O., & Mulloy, B. (2003). Sulfated fucans, fresh perspectives: Structures, functions, and biological properties of sulfated fucans and an overview of enzymes active toward this class of polysaccharide. *Glycobiology*, *13*, 29R–40R.

Blumenkrantz, N., & Asboe-Hansen, G. (1973). New method for quantitative determination of uronic acids. *Analytical Biochemistry*, *54*, 484–489.

Carpita, N. C., & Shea, E. M. (1988). Linkage structure of carbohydrates by gas chromatography-mass spectrometry (GC–MS) of partially methylated alditol acetates. In C. J. Biermann, & G. D. McGinnis (Eds.), *Analysis of carbohydrate by GLC and MS* (pp. 157–216). Boca Raton, FL: CRC Press.

Ciucanu, I., & Kerek, F. (1984). A simple and rapid method for the permethylation of carbohydrates. *Carbohydrate Research*, *131*, 209–217.

Dubois, M., Gilles, K. A., Hamilton, J. K., Revers, P. A., & Smith, F. (1956). Colorimetric method for determination of sugars and related substances. *Analytical Chemistry*, *28*, 350–356.

Freeman, E. E., Weiss, H. A., Glynn, J. R., Cross, P. L., Whitworth, J. A., & Hayes, R. J. (2006). Herpes simplex virus 2 infection increases HIV acquisition in men and women: Systematic review and meta-analysis of longitudinal studies. *AIDS*, *20*, 73–83.

Gerwig, G. J., Kamerling, J. P., & Vliegenthart, J. F. (1979). Determination of the absolute configuration of mono-saccharides in complex carbohydrates by capillary GLC. *Carbohydrate Research*, *77*, 1–7.

Green, L. C., Wagner, D. A., Glogowski, J., Skipper, P. L., Wishnok, J. S., & Tannenbaum, S. R. (1982). Analysis of nitrate, nitrite, and [15N]nitrate in biological fluids. *Analytical Biochemistry*, *126*, 131–138.

Harada, N., & Maeda, M. (1998). Chemical structure of antithrombin-active rhamnan sulfate from *Monostroma nitidum*. *Bioscience, Biotechnology, and Biochemistry*, *62*, 1647–1652.

Hayashi, T., & Hayashi, K. (1996). Calcium spirulan, an inhibitor of enveloped virus replication, from a blue-green alga *Spirulina platensis*. *Journal of Natural Products*, *59*, 83–87.

Hayashi, K., Nakano, T., Hashimoto, M., Kanekiyo, K., & Hayashi, T. (2008). Defensive effects of a fucoidan from brown alga *Undaria pinnatifida* against herpes simplex virus infection. *International Immunopharmacology*, *8*, 109–116.

Hoshino, T., Hayashi, T., Hayashi, K., Hamada, J., Lee, J.-B., & Sankawa, U. (1998). An antivirally active sulfated polysaccharide from *Sargassum horneri* (Turner) C. Agardh. *Biological & Pharmacutical Bulletin*, *21*, 730–734.

Kusaykin, M., Bakunina, I., Sova, V., Ermakova, S. P., Kuznetsova, T., Besednova, N., et al. (2008). Structure, biological activity, and enzymatic transformation of fucoidans from the brown seaweeds. *Biotechnology Journal*, *3*, 904–915.

Lee, J.-B., Hayashi, K., Hayashi, T., Sankawa, U., & Maeda, M. (1999). Antiviral activities against HSV-1, HCMV, and HIV-1 of rhamnan sulfate from *Monostroma latissimum*. *Planta Medica*, *65*, 439–441.

Lee, J.-B., Yamagaki, T., Maeda, M., & Nakanishi, H. (1998). Rhamnan sulfate from cell walls of *Monostroma latissimum*. *Phytochemistry*, *48*, 921–925.

Leiro, J. M., Castro, R., Arranz, J. A., & Lamas, J. (2007). Immunomodulating activities of acidic sulphated polysaccharides obtained from the seaweed *Ulva rigida* C. Agardh. *International Immunopharmacology*, *7*, 879–888.

Liu, J., & Pedersen, L. C. (2007). Anticoagulant heparan sulfate: Structural specificity and biosynthesis. *Applied Microbiology and Biotechnology*, *74*, 263–272.

Nagasawa, K., Inoue, Y., & Tokuyasu, T. (1979). An improved method for the preparation of chondroitin by solvolytic desulfation of chondroitin sulfates. *Journal of Biochemistry*, *86*, 1323–1329.

Nakamura, T., Suzuki, H., Wada, Y., Kodama, T., & Doi, T. (2006). Fucoidan induces nitric oxide production via p38 mitogen-activated protein kinase and NF-kB-dependent signaling pathways through macrophage scavenger receptors. *Biochemical and Biophysical Research Communications*, *343*, 286–294.

Palú, G., Benetti, L., & Calistri, A. (2001). Molecular basis of the interactions between herpes simplex viruses and HIV-1. *Herpes*, *8*, 50–55.

Petersen, B. O., Vinogradov, E., Kay, W., Würtz, P., Nyberg, N. T., Duus, J. Ø., et al. (2006). H2BC: A new technique for NMR analysis of complex carbohydrates. *Carbohydrate Research*, *341*, 550–556.

Preeprame, S., Hayashi, K., Lee, J.-B., Sankawa, U., & Hayashi, T. (2001). A novel antivirally active fucan sulfate derived from an edible brown alga, *Sargassum horneri*. *Chemical & Pharmaceutical Bulletin*, *49*, 484–485.

Silvestri, L. J., Hurst, R. E., Simpson, L., & Settine, J. M. (1982). Analysis of sulfate in complex carbohydrates. *Analytical Biochemistry*, *123*, 303–309.

Stevenson, T. T., & Furneaux, R. H. (1991). Chemical methods for the analysis of sulphated galactans from red algae. *Carbohydrate Research*, *210*, 277–298.

Sweet, D. P., Shapiro, R. H., & Albersheim, P. (1975). Quantitative analysis by various g.l.c. response-factor theories for partially methylated and partially ethylated alditol acetates. *Carbohydrate Research*, *40*, 217–225.